Physical aging effect on viscoelastic behavior of polymers

S.G. Nunes, R. Joffe, N. Emami, P. Fernberg, S. Saseendran, Antonella Esposito, S.C. Amico, J. Varna

Composites Part C: Open Access 7 (2022) 100223

Contents lists available at ScienceDirect

Composites Part C: Open Access

journal homepage: www.sciencedirect.com/journal/composites-part-c-open-access

Physical aging effect on viscoelastic behavior of polymers

S.G. Nunes [a,d,e,*], R. Joffe [a], N. Emami [a], P. Fernberg [a], S. Saseendran [a,b], A. Esposito [c], S. C. Amico [d], J. Varna [a,e]

[a] Department of Engineering Sciences and Mathematics, Luleå University of Technology, Luleå, Sweden
[b] Department of Polymer Materials and Composites, Research Institutes of Sweden, Piteå, Sweden
[c] Normandie Univ, UNIROUEN, INSA Rouen, CNRS, Groupe de Physique des Matériaux, 76000 Rouen, France
[d] Materials Engineering Department, Federal University of Rio Grande do Sul, Porto Alegre, Brazil
[e] Institute of Mechanics and Mechanical Engineering, Riga Technical University, Riga, Latvia

ARTICLE INFO

Keywords:
Physical aging
Viscoelasticity
Shift factors
Numerical analysis

ABSTRACT

The effect of physical aging on the viscoelastic (VE) behavior of epoxy resin is investigated experimentally performing strain-controlled tests at various temperatures on specimens aged at different temperatures (T_A) for different times (t_A). The aging effect is analyzed using as a framework Schapery's type of thermo-aging-rheologically simple (T-A-R simple) VE model that contains aging-state and test-temperature dependent shift factor. Experiments show that in first approximation, the shift factor can be presented as the product of aging related shift factor a_A and temperature related factor a_T. It is found that for short aging times the change rate of the aging shift factor with t_A does not depend on T_A, whereas for long $t_A$at high T_A the rate increases. Shift factors alone are not able to explain differences in relaxation curves for almost "fully" aged specimens aged at different high T_A, It is shown that a T-A-R complex VE model with two additional aging-dependent functions can describe the observed discrepancies.

1. Introduction

Thermoset resins are widely used as matrix in fiber reinforced polymeric composites for high performance applications. For long-term performance design, it is necessary to understand the viscoelastic-viscoplastic response of the composite. Since polymer is the viscoelastic (VE) component of many composites, a typical epoxy resin is the subject of this study. During the service life, epoxy resins are used below their glass transition temperature (T_g). This means that they are not necessarily in a thermodynamic equilibrium state and that local molecular motions, which are temperature and time dependent may cause a phenomenon known as physical aging [1].

Physical aging is the direct consequence of the intrinsically out-of-equilibrium state of glassy amorphous polymers [2], it occurs at any temperature below the glass transition and produces significant variations of the specific volume and enthalpy in the attempt of reaching an equilibrium state. It is reasonable to assume that physical aging is accompanied by changes in the polymer mechanical and viscoelastic properties and, consequently, becomes a concern for industries [3].

Parvatareddy at al. [4] investigated thermoplastic polymers reinforced with carbon fibers and concluded that physical aging caused an increase in modulus and brittleness, attributing it to densification of the polymer with aging time. They also reported that in several composite systems physical aging retards the creep process and causes a general decrease in properties. Mckenna [5] stressed that the non-equilibrium nature of glassy polymers and the physics behind aging are important in developing constitutive equations describing the volume/temperature/stress time response of polymer-based materials. Arnold [6] studied the effect of physical aging on polystyrene's properties and found that long-term physical aging significantly shortens the creep rupture time and decrease the strain to failure. Studying the effect of physical aging on the fracture behavior of crosslinked epoxies, Truong and Ennis [7] reported an increase in the yield stress as the main contributor to the reduction in fracture toughness. Other authors [8–9] reported a decrease in fracture resistance associated with embrittlement as well as an increase in Young modulus and strength.

As physical aging takes place simultaneously with creep and stress relaxation, interpreting and predicting the long-term behavior of a viscoelastic material cannot be done without taking physical aging into account. The constantly evolving properties may strongly impair the

* Corresponding author.
E-mail address: stephanie.goncalves-nunes@rtu.lv (S.G. Nunes).

https://doi.org/10.1016/j.jcomc.2021.100223
Received 1 September 2021; Received in revised form 7 December 2021; Accepted 20 December 2021
Available online 21 December 2021

long-term viscoelastic behavior through significant shift in the time scale [10–11]. Besides, physical aging accelerates as the service temperature approaches the glass transition and, therefore, the effect of physical aging on the viscoelastic behavior should be evaluated as a function of temperature. According to Lee and McKenna [9], the magnitude of the change in mechanical properties upon aging depends on the distance of the initially out-of-equilibrium system from the thermodynamic equilibrium. Physical aging can be reversed [10,12] by annealing the specimen at $T>T_g$ to reach a higher-energy state and erase any possible thermal history (rejuvenation). It is followed by rapid quenching to $T<T_g$, then keeping the polymer in isothermal conditions ($T_A = const$) for different times (t_A), and finally quantifying the enthalpy overshoot associated with structural relaxation upon heating through the glass transition [1,8,13-14]. Many researchers use viscoelastic creep or stress relaxation tests and combine the time-temperature superposition principle (TTSP) with an aging superposition, introducing thermo-aging-temperature superposition principle [8,14-15]. In particular, they build master curves and use the concept of effective time theory (ETT), proposed by Struik [10], which assumes that all retardation times are equally affected by aging with constant aging shift rate.

For this purpose, ETT concept presumes that to predict a data and analyze all material momentary response the test times need to be shorter than the aging time. This snapshot assumption, were the maximum testing time after aging is equal to $t_A/10$, assuming that no significant aging occurs during each test, is adopted by majority of the researchers in this field [5,8,9,13-18]. In this methodology, before introducing the effective time (λ), the slope of the shift factor vs. aging time curve, is used to find the aging shift factor for a full aging time, Pierik et al. [19], performed creep tests under several testing temperatures on poly(phenylene sulfide) composites reinforced with carbon woven fabric. Creep rate predictions after correcting, using ETT, for the influence of physical aging were improved. Bradshaw and Brinson [20] affirmed that the cornerstone of long-term predictive schemes for linear VE behavior is the ETT and reported a continuous change in compliance and modulus as the material evolves towards equilibrium, using aging-time superposition principle to explain data.

The objective of this paper is to assess the effect of physical aging on VE behavior of an epoxy resin, based on linear VE model with parameters, such as coefficients in Prony series (C^m) and temperature and aging shift factors (a_T and a_A). This research proposes a different methodology, not based on ETT, for testing and parameter determination in the model. The experimental aging effect study is performed using as a framework a thermo-aging-rheologically simple (T-A-R simple) viscoelasticity model, demonstrating its applicability and pointing out its limitations. In this model, only the shift factor is affected by aging and test temperature and the shift factor is presented as a product of two terms, one related to aging (a_A) and one (a_T) related to the testing temperature. Even if this model succeeded in describing most of the experimental results, some limitations were observed: a) the aging temperature T_A affects both the aging and temperature shift factors; b) the slope of the aging shift factor vs. aging time, which is assumed independent on T_A by several authors [3,9,10], actually increases with increasing T_A. A rheologically complex model, never used to simulate physical aging effect before, is outlined to account for this behavior.

2. Theoretical considerations

2.1. Thermo-aging-rheologically simple viscoelastic model

A thermodynamically consistent, linear VE model [21] is used in this study. Parameter β in equations represents the aging state that depends on aging time and temperature. This parameter may be changing during the loading history. Viscoplastic effects are not considered.

The main model assessed in this paper for its applicability to the used epoxy resin is thermo-aging-rheologically simple (T-A-R simple). The derivation of a more general thermo-aging-rheologically complex (T-A-R complex) model based on expansion of Helmholtz free energy follows the path presented in [22,23]. In T-A-R simple materials, the test temperature and the aging state affect the shift factor only. In this work, the constitutive law for a T-A-R simple material is taken from [24]. It is written in 1-D formulation because all mechanical experiments were performed in uniaxial tensile loading

$$\sigma(t) = E_r\varepsilon + \int_0^t \Delta C(\psi-\psi')\frac{d(\varepsilon)}{d\psi'}d\psi' \tag{1}$$

$$\Delta C(\psi) = \sum_{m=1}^{M} C^m exp\left(-\frac{\psi}{\tau_m}\right) \tag{2}$$

In (1) and (2), σ and ε are time t dependent stress and strain, τ_m are relaxation times and E_r is the rubbery modulus. Coefficients in Prony series C^m are constants that do not depend on test temperature T and aging. The reduced time ψ is defined by expression

$$\psi(t) = \int_0^t \frac{1}{a(\beta,T)}d\zeta \tag{3}$$

The shift factor a in (3) depends on temperature T and the state of aging represented by β.

An assumption (to be verified) is made that, with accuracy sufficient for practical applications, the shift factor a in (3) can be written as a product of a temperature (T)-dependent term (a_T) and an aging (A)-dependent terms

$$a(\beta,T) = a_A(\beta)a_T(T) \tag{4}$$

Any free expansion strains, ε_{free} from unconstrained hygro-thermal or physical aging related dimensional changes are not explicitly included in (1), which means that the strain ε in the loading direction is

$$\varepsilon = \varepsilon_{applied} - \varepsilon_{free} \tag{5}$$

As described in Section 3, mechanical tests were performed under different isothermal conditions ($T = const$ in each test). The mechanical test length was selected to ensure that during the test the change of the aging state is negligible. Since during the mechanical test β and Twere constant, both a_A and a_T are also constant and (3) can be written as

$$\psi(t) = \int_0^t \frac{1}{a_A(\beta)a_T(T)}d\zeta = \frac{t}{a_A(\beta)a_T(T)} \tag{6}$$

In the particular case of an idealized relaxation test, the strain ε_0 is applied at $t = 0$ as a Heaviside step function and the stress relaxation according to (1), (2) and (6) is given by

$$\sigma_{rel} = \varepsilon_0\left[E_r + \sum_{m=1}^{M} C^m exp\left(-\frac{\psi}{\tau_m}\right)\right], \quad \psi = \frac{t}{a_A a_T} \tag{7}$$

In (7) only the parametersa_A and a_T depend on T and β that are constant during the test. The expression in brackets is the stress relaxation function and its value at $t = 0$ is the glassy modulus of the epoxy resin. Eq. (7) together with (non-ideal) relaxation test data is often used to find the coefficients C^m in Prony series.

2.2. L-H test to determine Prony coefficients

In real testing conditions, the strain cannot be applied as a Heaviside step-function. In a strain-controlled test, the strain increases from zero to ε_0 over finite time t_1. Therefore, at least during the 2–4 times larger interval, the recorded data and Eq. (7) are not compatible, and the Prony coefficients corresponding to short relaxation times cannot be obtained. In this work, a loading ramp, called L-H test, is applied to determine Prony coefficients. The L-H test is under strain control and consists of two steps. In the first step, identified as L(t_1)-step, the strain linearly grows during time t_1 from zero to a selected value ε_0. This step is followed by a holding step (H(t^*)), during which the strain is held constant

for t^* min.

Simple analytical expressions for the stress dependence on time in both steps can be derived from (1). For the L-step follows

$$\sigma(t)=\varepsilon_0\left[E_r\frac{t}{t_1}+\frac{a_T a_A}{t_1}\sum_{m=1}^{M}C^m\tau_m\left(1-exp\left(-\frac{t}{\tau_m a_T a_A}\right)\right)\right],\ \varepsilon=\varepsilon_0\frac{t}{t_1},\quad 0<t\le t_1 \tag{8}$$

In the H-step, where the strain is held constant, $\varepsilon=\varepsilon_0$ the solution is

$$\sigma(t)=\varepsilon_0\left[E_r+\frac{a_T a_A}{t_1}\sum_{m=1}^{M}C^m\tau_m exp\left(-\frac{t}{\tau_m a_T a_A}\right)\left(exp\left(\frac{t_1}{\tau_m a_T a_A}\right)-1\right)\right],\quad t_1<\ t\le t_1+t^* \tag{9}$$

Eqs (8) and (9) are linear with respect to Prony coefficients C^m. The least-square method was used to fit the experimental L-H test data at fixed temperature T and aging state β. All coefficients have to be non-negative, i.e. $C^m \ge 0$, $m = 1, 2, ..., M$. In this ramp, there is no need for very high strain rates to get close to the ideal relaxation test conditions, the strain increase can be better controlled and, hence, a more accurate VE response description for short testing times is obtained [25].

2.3. Incremental simulation procedure for arbitrary ramps

The strain dependence on time in tests may be more complex than the linear L-step and the constant H-step in the L-H test described by equations in Section 2.2 Indeed, the strain rate in the uploading step may be not exactly constant if the loading is cross-head displacement controlled, and in the constant strain H-step the temperature may vary or the aging state change. The ramp can be different, for example, the H-step may be followed by strain-controlled unloading (U-step) etc. All these "deviations" make Eqs. (8) and (9) invalid.

To use the material model (1), (2) and (3) in arbitrary loading ramps an incremental formulation of the T-A-R complex model called VisCoR, developed in [22,23] and used in [25], will be applied. In this paper, was used a T-A-R simple version of the incremental expressions. Simulations using the incremental procedure will be performed in Section 4 to determine the dependence of the aging-related shift factor a_A on the aging time t_A, and in Section 5 to simulate validation cases using recorded strain versus time ramps.

3. Material, manufacturing and test routines

3.1. Material and manufacturing

In this study the cold-curing epoxy system Araldite® LY 5052/Aradur® HY 5052, provided by Hunstsman, was used. This resin system has low viscosity and long pot-life. The resin was mixed during 5 min with the hardener in a proportion of 100:38 by weight, and then the specimens were casted in a silicone mold and degassed for approximately 12 min in a vacuum system. After curing at room temperature (RT) ≈ 23 °C for 24 h, the specimens were demolded and post-cured at 105 °C for 4 h, to obtain fully cured samples (degree of cure $DoC = 0.992$, determined by Kamal's model [24]). After grinding and polishing, the rectangular specimens had dimensions 160 × 15 × 4 mm^3. The T_g of the produced specimens was around 130 °C .

3.2. Testing philosophy in quasi-static tensile tests

Since this study aims to analyze the effect of physical aging on VE behavior, the specimens were aged at selected constant temperature T_A. The viscoelastic response after aging for a time t_A was measured in L-H test at the same temperature. After additional aging, the specimen was tested again. The total aging time for a specimen was at least 5000 min. The used aging temperatures were in the region between 70 °C and 110 °C . The selected temperature range corresponds to the expected application range of epoxy matrix composites. The recorded stress dependence on time allowed determination of the aging shift factor a_A dependence on the aging temperature T_A and time t_A.

The L-H quasi-static tensile tests were performed using an Instron Universal 3366 machine, with load cell of 10 kN and mechanical grips, the distance between grips was 100 mm. The axial strain was measured using a standard Instron 2620–601 dynamic extensometer, with a 50 mm gage length. The time, strain and load acquisition rate were 1 Hz. All the tests were performed in strain-control mode. The L(t_1)-H(t^*) test consisted of two steps: loading to ε_0 in $t_1 = 1$ min with a constant strain rate (L-step) followed by holding at ε_0 (H-step) for t^* min. The maximum strain in tests was $\varepsilon_0 = 0.5\%$, except for the tests at $T = 110°C$, where the value was reduced to $\varepsilon_0 = 0.3\%$ to avoid development of viscoplastic strains. In the H-step, the stress relaxation was recorded. After unloading, strain recovery was recorded in order to ensure that the strain is reversible. For the used epoxy resin and test conditions, the mechanical response was reversible and strains fully recovered in time interval $10t^*$ [25].

The change in the VE response of a specimen due to aging is not much larger than the observed differences in behavior between different specimens. Therefore, as much as possible data has to be obtained from the same specimen. The same specimen was used during the whole aging process and the specimen was not removed from the testing machine until all the steps of the program (aging, mechanical testing, repeated thermal rejuvenation, see Section 3.4) were complete. This approach was introduced and detailed in a previous work [25]. Thus, from each specimen it was possible to obtain T-related relaxation master curves and Prony coefficients covering a large time span, the a_T dependence on temperature, as well as the aging shift factor a_A dependence on the aging time t_A at a given aging temperature T_A. Obviously, the relevance of the trends and relationships found with this approach was verified using several specimens.

3.3. Thermal rejuvenation of epoxy specimens

As physical aging is a thermo-reversible phenomenon, rejuvenation can be achieved by annealing. Prior to any experimental program, annealing was performed to erase the thermal history of the glassy epoxy resin. For some specimens, annealing followed by the whole test program was repeated several times, and during the entire process, the specimen was never removed from the testing machine, neither the grips released nor re-tightened. Annealing was performed by mounting the specimen on the testing machine, which was equipped with an Instron environmental chamber 3119–406, then heating above the glass transition ($T = T_g + 20$ °C = 150 °C) holding zero load and keeping the system in isothermal conditions for 40 min. The annealing temperature and time were selected based on the results reported in previous works [9, 10, 13]. After annealing, the chamber was switched off, the door was opened and the specimen cooled down holding zero load to RT ≈ 23 °C. The accuracy of the temperature displayed on the control panel of the chamber was verified with a thermocouple, placed close to the specimen, both measurements providing a very similar T vs. t curves for the thermal rejuvenation process (heating and cooling steps). The annealing and cooling-down process was the same for all specimens, also when the entire program was repeated on the same specimen several times.

3.4. Viscoelastic response as a function of t_A at fixed T_A

After rejuvenation the aging temperature T_A was selected, the extensometer was attached and the machine was used in load-control mode with zero force to enable free expansion during the heating-up. It took about 20 min to reach and stabilize the target temperature and to start the first L-H test. Considering the recorded heating history, it was estimated that, by the time the test started, the specimen was aged for approximately $t_A = 20$ min.

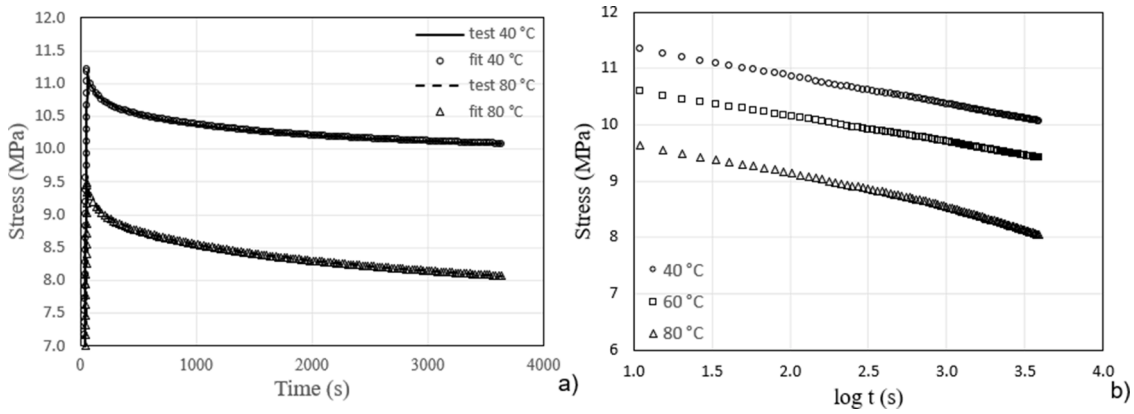

Fig. 1. Stress relaxation for "A-ref" Sp10 ($T_A = 80^{\circ}C, t_A = 5466$ min): a) experimental stress curves and fit in L-H(60 min) test with $\varepsilon_o = 0.5\%$ at T=40 °C and 80 °C; b) simulated stress relaxation curves in ideal relaxation test at $\varepsilon_o = 0.5\%$at three testing T.

Then, a strain-controlled L-H test was performed at T_A. Hence, during the test and during the strain recovery after unloading the aging continued. The time until the next L-T test was long enough to allow for VE recovery and for additional aging. The holding time t^* in the $H(t^*)$-step was selected based on the reached t_A ensuring that during the L-H test the aging state would not significantly change (a constant value of a_A during the entire test is assumed in (8), (9)). This implies that with increasing t_A a larger holding time $t^*$was used, similarly as in [20] where the used test times were much shorter than the aging time.

The aging was continued for approximately 5000 min, except for one specimen that was aged at 100 °C for more than 10,000 min. After 5000 min of aging the VE response change with aging time, expressed in terms of the shift factor, was very slow: the shift factor change during last 3000 min was approximately 5% of the change between 20 and 100 min of aging. Therefore, this aging state was defined as a reference state for aging shift a_A determination.

The procedure described in this section was performed at different aging temperatures. For some specimens, after finishing the test program the extensometer was removed but the grips were not released, and a new annealing was performed as described in Section 3.3. The rejuvenated specimen was then used in a new test program either at the same or at a different T_A. One to three specimens were tested at each T_A. In following, each specimen is identified as "SpN ", with relevant information including testing T, aging time t_A and temperature T_A. The routine to determine the aging related shift factor a_A is described in Section 4.2.

3.6. Time-temperature shift and master curves for aged specimens

After the final aging step, the L-H test showed small changes in the peak stress comparing with the previous test and decision was made that the specimen is sufficiently aged to undergo no further noticeable change in its aging state during the following T-shift tests described below. To verify that, one more t_A data "point" was obtained for the specimen, corresponding to an additional aging for 1000 min. This aging state for the specimen was used as a reference, indicating it as "A-ref".

The construction of the T-shift master curve for the "A-ref" specimen required L-H tests at several temperatures. To minimize additional aging, temperatures below the used aging temperature were used ($T \leq T_A$) and the holding part (H) in the L-H test t^* was 60–120 min. In the following, this will be noted as H(60 min) or H(120 min). For example, for a specimen aged at $T_A = 90^{\circ}C$ the tests were performed at 40, 60, 80 and 90 °C. The strain recovery was accelerated by performing it at 10 °C higher temperature than the test temperature, but only if it was lower than the previously used T_A.

The routine to determine the temperature-related shift factor a_T, to build the master curve and to calculate Prony coefficients is described in Section 4.1.

4. Data reduction methodology

4.1. Master curves, T-shift factors

In the T-A-R simple model used in this work, only the horizontal shift in log$t$ axis of the ideal Heaviside relaxation test data, is used to construct the relaxation master curves with respect to the reference temperature T_{ref}. However, the L-H test of "A-ref" specimens is not an "ideal" relaxation test and therefore the routine was changed accordingly. The following steps illustrate the routine using as an example "A-ref" Sp10 aged at 80 °C:

A Prony coefficients from L-H test:

The stress curve recorded in L-H(60 min) test at a given T is used to find Prony coefficients using (8) and (9). Since the shift factors are not known, it is assumed that $a_T = a_A = 1$. Hence, the Prony coefficients, obtained using the method of least squares with additional thermodynamics dictated condition that all coefficients have to be non-negative, can be used only for this temperature. For tests at different test temperatures the Prony coefficients are different. This procedure ensures high accuracy, as shown in Fig. 1a, Prony coefficients are given in Table 1.

A Master curves

Prony coefficients in Table 1 were used in (7) to simulate stress relaxation in a Heaviside step-loading at the same temperature as the initial L-H test (Fig. 1b).

Table 1
Prony coefficients C^i (MPa) from fitting L-H(120*min*) test data for "A-ref" Sp10, $T_A = 80^{\circ}C, t_A = 5466$ min at three temperatures, $E_r = 0$.

(s)	10^{-1}	10^{0}	10^{1}	10^{2}	10^{3}	10^{4}	10^{5}	10^{6}	10^{7}
40 °C	0	517.0	104.3	96.8	103.0	0	747.5	1297.8	0
60 °C	0	251.2	103.4	86.3	95.2	0	736.7	1177.1	0
80 °C	0	279.1	101.8	95.7	124.1	45.9	1637.8	0	0

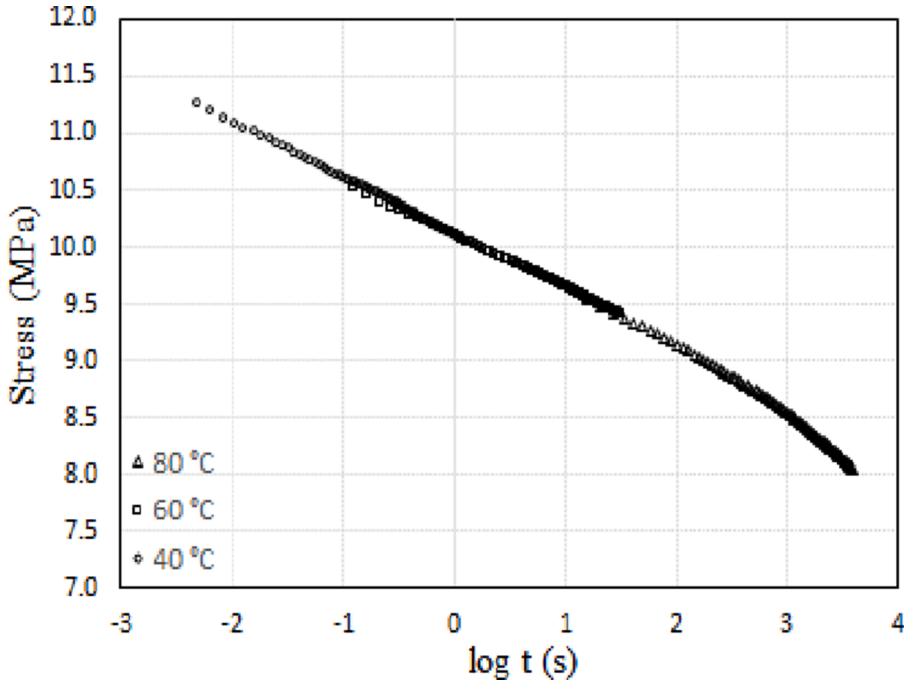

Fig. 2. Stress relaxation master curve for "A-ref" Sp10 ($T_A = 80^{\circ}C$,t_A = 5466 min) at $\varepsilon_o = 0.5\%$ and $T_{ref} = 80^{\circ}C$.

Then, the stress relaxation curves in Fig. 1b were shifted horizontally to obtain master curve corresponding to $T_{ref} = 80^{\circ}C$. Shifting was performed using two alternative techniques a) visual, using EXCEL; b) using a homemade misfit minimization code written in MATLAB. To ensure reliable results, the pair of considered curves should have an overlapping stress region. During visual shifting, the reliability of the master curve depends on the experience of the operator. After the shift, the pair of curves never perfectly coincide in the overlapping region. The main advantage of visual shifting is that the operator sees the "bigger picture", not only the overlapping region.

To provide a more consistent analysis of the data, with results not varying from user to user or from one data set to another data set, a MATLAB code was developed as an alternative to "visual" shift. Similar procedure was outlined in [20,26]. The authors used error minimization to find shift factors and master curve.

In this code, first, an overlapping stress region of two adjacent curves is identified. Since log$t$ scale is used, the number of data points in these two shifted curves in the overlapping region is different and, therefore, point-by-point summation of squares of stress deviations is not possible. Instead, stress vs. log$t$ data from both curves (tests at two different temperatures T_1 and T_2) in the overlapping region $\sigma \in [\sigma_s,\sigma_f]$ are approximated by liner functions $y_1 = k_1x + b_1$ (for T_1) and $y_2 = k_2x + b_2$ (for T_2). By inversion these functions can be expressed as $x_1 = (y - k_1)/b_1$ and $x_2 = (y - k_2)/b_2$ respectively. The distance between these two curves can be changed by introducing the shift parameter a_T, which allows shifting the x_2- curve towards the x_1- curve by rewriting x_2 as $x_{2sh} = \frac{(y-k_2)}{b_2} - \log a_T$. A good measure for minimizing the distance between adjacent curves is $\min_{a_T} \int_{\sigma_s}^{\sigma_f} [x_{2sh}(y) - x_1(y)]^2 dy$. Substituting the above expressions for $x_1(y)$ and $x_{2sh}(y)$, then integrating and finding minimum with respect to a_T, the following expression is obtained

$$\log a_T = -\frac{b_2}{k_2} + \frac{b_1}{k_1} - \frac{\sigma_s + \sigma_f}{2}\left(\frac{1}{k_1} - \frac{1}{k_2}\right) \tag{10}$$

The loga_T value obtained by "visual" fitting is 2.1 between 60 °C to 80 °C and 1.4 between 40 °C to 60 °C. The MATLAB code provided with (10) almost identical values (2.124 and 1.471 respectively). The stress relaxation master curve at $T_{ref} = 80^{\circ}C$ is shown in Fig. 2.

Finally, the method of least squares was applied to the data shown in Fig. 2 ("master-data" for $T_{ref} = 80^{\circ}C$) to find Prony coefficients (Table 2). These coefficients together with a_T and the aging shift factor a_A define the VE model that can be used for simulations of arbitrary temperature- and aging-dependent loading ramps.

4.2. Shift factor a_A related to physical aging

The starting point in data reduction for each specimen is selecting the aging state at the end of the performed aging as a reference ("A-ref"). The same Sp10 as in Section 4.1 is used as an example for data reduction with respect to physical aging. The Prony coefficients (Table 2) and the shift factor a_T for the "A-ref" state at $T_{ref} = 80^{\circ}C$ are used to simulate the L-H test for different states of aging i.e. after different aging times at the aging temperature $T_A = 80^{\circ}C$, using in simulations the shift factor loga_A as a parameter. Since in this case $T_A = T_{ref}$, the $a_T = 1$ (log$a_T = 0$).

The incremental VisCoR code [25] was used to simulate the L-H tests corresponding to different aging times t_A. In VisCoR simulations, the data points for time and strain were taken from the experimental records and the shift parameter a_A was used as a variable. To minimize the difference between the simulated and experimental stress curves, the sum of deviation squares for all points was minimized using the shift factor. Since the time instants in test and simulations were exactly the same, the minimization procedure was rather simple.

The optimized (with respect to a_A) simulation results and

Table 2
Prony coefficients of the master curve, C^i (MPa), for Sp10.

τ_m (s)	0.01	10^{-1}	10^{0}	10^{1}	10^{2}	10^{3}	10^{4}	10^{5}	10^{6}	10^{10}
C^i	93.1	102.4	99.4	86.6	104.9	111.8	267.8	0	0	1425.4

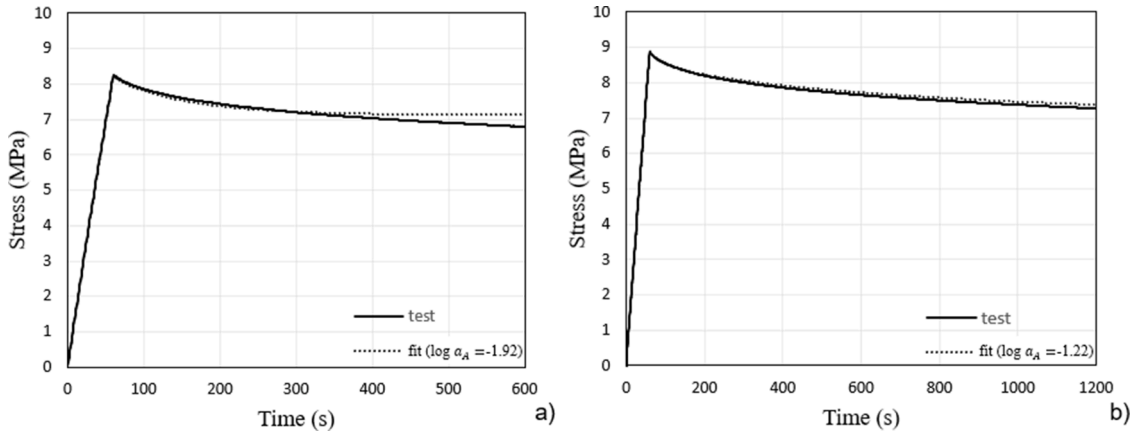

Fig. 3. Stress response for Sp10 in L-H test with $\varepsilon_o = 0.5\%$ at T_A=80 °C: a) after $t_A = 20$ min and b) $t_A = 155$ min.

Table 3
Aging shift factor $\log a_A$ dependence on t_A at $T_A = 80^\circ C$ for Sp10. The state after $t_A = 5466$ min of aging is assumed as a reference.

Aging time (min) 1st annealing	20	155	444	2502	5466
$\log a_A$	−1.92	−1.22	−0.92	−0.07	0.00

experimental results in a test that started after $t_A = 20$ min of aging are shown in Fig. 3a and for a test that started after $t_A \approx 155$ min of aging in Fig. 3b. The best-fit shift factors $\log a_A$ from these tests are −1.92 and −1.22, respectively. In Fig. 3a the agreement between tests and simulation is very good only for $t < 300s$, whereas in Fig. 3b it is good over a much larger time interval. The reason for the inaccurate simulation in Fig. 3a is the very low value of $a_A \approx 0.01$ ($\log a_A = -1.92$). The master curve in Fig. 2, which was used to obtain Prony parameters, is based on data for $t < 3600s$ with $a_T = a_A = 1$. Hence, the applicable time interval based on these data does not exceed $t < 10,000s$. Now, when $a_A \approx 0.01$ the time interval "shrinks" to $t < 0.01*10,000s = 100s$. The situation is similar as in VE tests at different temperatures, i.e. the stress relaxation behavior at lower temperature is useful for predicting the VE behavior only for a much shorter time interval at higher T. The above explanation is confirmed in simulations and tests corresponding to longer aging times, for example, $t_A \approx 155$ min shown in Fig. 3b ($a_A \approx 0.06$). Hence, the master curve tests for the "A-ref" specimens should have been built with a longer holding time than the 60 min actually used.

Finding the best fit, the minimization was used only in the applicable time interval estimated as described above. The process was iterative (2–3 iterations). First, the response in the whole test interval was simulated and the obtained best fit was used to get the first estimate of a_A. Based on the estimated a_A, a valid time interval Δt for fitting was selected and the fitting procedure repeated. The a_A for the best fit was almost independent on the length of the fitting interval if it was shorter than the Δt. For example, fitting over the first 200 s or 300 s in the case shown in Fig. 3a, would lead to a difference of 0.01 in the $\log a_A$ value.

For larger t_A, the value of $\log a_A$ approaches zero and predictions are good over the entire time interval 60 min. The values of the aging shift factors, determined with respect to the aging state after $t_A = 5466$ min, are shown in Table 3.

5. Results and discussion

5.1. Repeatability of tests

In a strain-controlled ramp with linearly increasing strain to 0.5%, the stress values $\sigma_{0.5\%}$ at the end of the L-step for four specimens (Sp1 to Sp4) are 11.09, 11.78, 12.96 and 13.17 MPa. Directly after post curing the tests were performed at test temperature 30°C with strain rate

Table 4
Stress, $\sigma_{0.5\%}(MPa)$, reached at 0.5% strain, strain rate 0.5%/min, in two identical tests at different constant temperatures.

Specimen/test	Sp 8			Sp 9		
	30°C	50°C	70°C	40°C	60°C	80°C
test 1	12.49	10.94	9.70	13.76	11.67	10.23
test 2	12.42	10.94	9.81	13.74	11.67	10.45

0.05%/min. The scatter between different specimens is rather high. When the test is repeated four times on the same specimen (Sp1), removing it from the testing machine during strain recovery, the $\sigma_{0.5\%}$ values are 11.36, 10.88, 11.09 and 12.08 MPa. The scatter is smaller but still approximately 10% of the reached stress value.

As shown in Table 4, the results are more stable if, following the routine described in Section 3.2, in-between the consecutive tests the grips are not released.

The repeatability of the VE response after rejuvenation was investigated. After finishing the aging and mechanical testing program, the specimen was annealed as described in Section 3.3 and the aging and testing program was repeated. An example showing the extremely high repeatability is shown in Fig. 4. For the same aging time t_A, the stress relaxation curves, corresponding to the 2nd and the 1st annealing almost coincide.

The results prove that annealing is an efficient process enabling VE repeatability of the specimen. Even after four rejuvenations, the epoxy specimen did not change its behavior.

5.2. Shift factors related to aging (a_A) and test temperature (a_T)

The analysis started with the temperature shift factor a_T. A specimen, see Section 3, aged at a given temperature T_A for $5000 < t_A < 6000$min was used as a "A-ref" specimen in L-H tests at different temperatures to gather data for constructing master curves and determining the temperature shift factors a_T, following the procedure described in Section 4.1 using automated data shifting. The values of $\log a_T$ obtained during the construction of the master curves are presented in Figure 5 showing data for three specimens aged at the same temperature $T_A = 80^\circ C$. Figure 5b reports the shift factors for specimen Sp11. After aging and testing at one temperature, the specimen was rejuvenated, then aged and tested again at different temperature.

A rather unexpected trend is observed in Fig. 5b: the $\log a_T$ dependence on T has a rate affected by the aging temperature. The slope is the steepest for the lowest $T_A = 70^\circ C$. The difference between aging at 80°C and 90°C is small, comparable with the scatter between different specimens in Fig. 5a. If this trend is confirmed in future investigations, the applicability of (4) and (6) for loading ramps with arbitrary evolution of

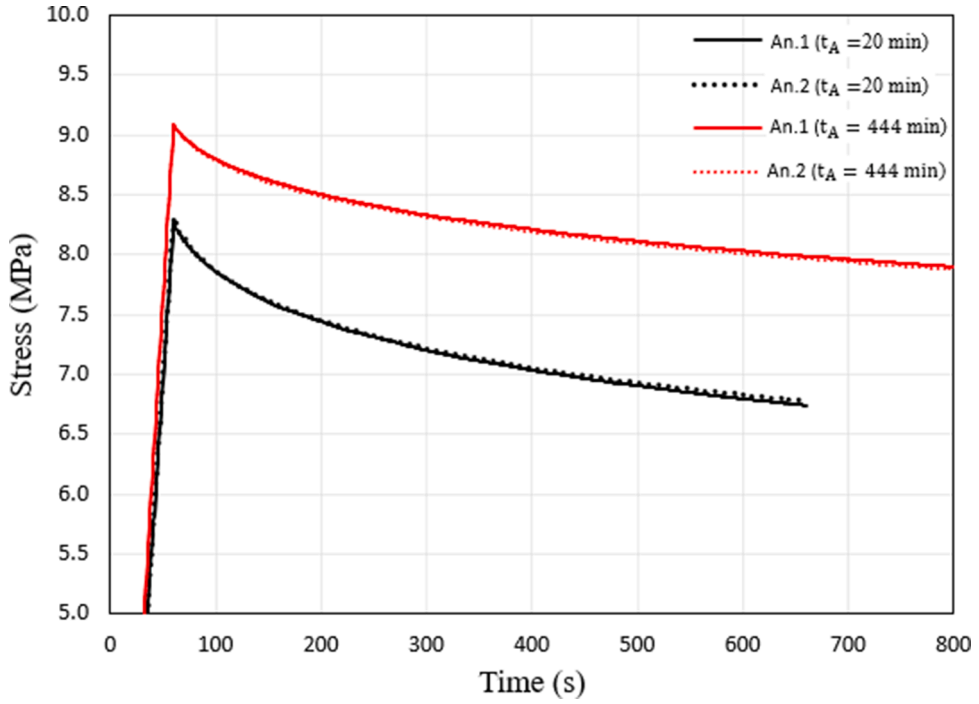

Fig. 4. Repeatability of stress relaxation for Sp10 in L-H test after 2nd annealing (An.2) compared with the same test after 1st annealing (An.1). Mechanical tests with $\varepsilon_o = 0.5\%$at $T = T_A = 80^{\circ}C$ corresponding to two aging times t_A.

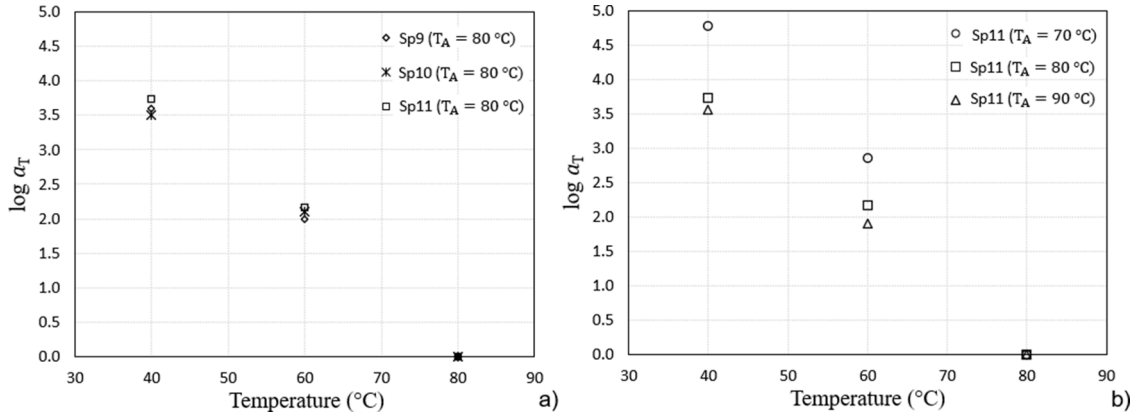

Fig. 5. Temperature shift factor a_T vs. temperature for master curves built at $T_{ref} = 80^{\circ}C$ using "A-ref" specimens: a) three specimens aged at $T_A = 80^{\circ}C$ and b) the same specimen aged at three different T_A.

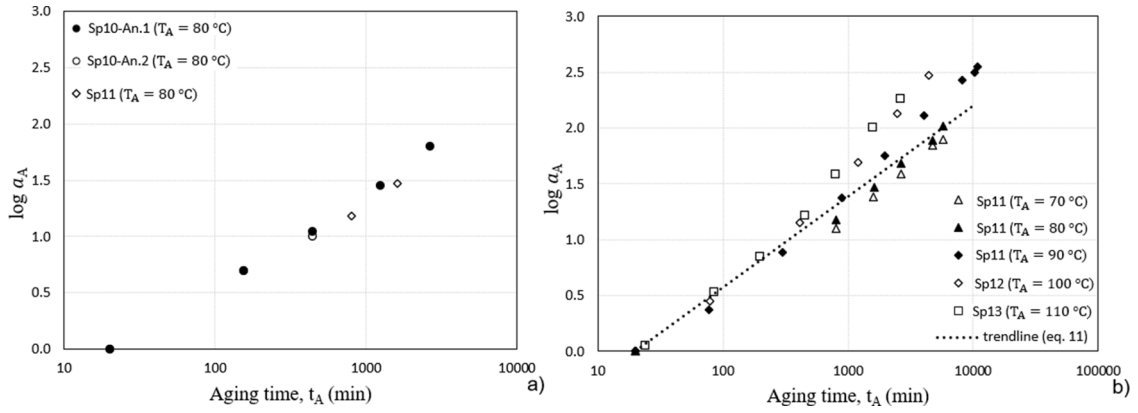

Fig. 6. Dependence of the aging shift factor a_A on T_A and t_A: a) two specimens aged at $T_A = 80^{\circ}C$; b) all data showing quasi-linear (constant rate) behavior at short aging times.

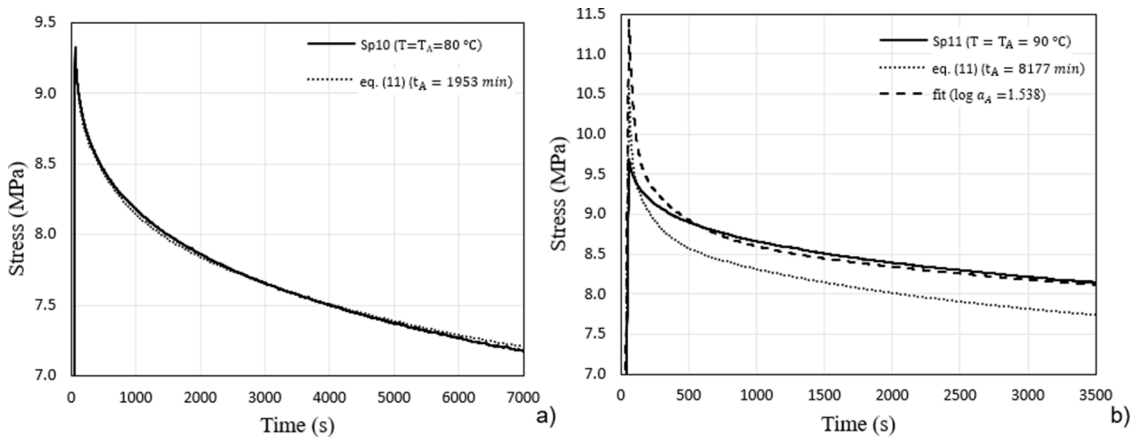

Fig. 7. Simulated and experimental stress response in L-H test ($\varepsilon_0 = 0.5\%$) at different aging states. Prony coefficients obtained at t_{A0} were used to simulate the test for the same aging temperature T_A but different t_A. The shift factor change was calculated using (11) for a) $t_{A0} = 78$ min and b) $t_{A0} = 301$ min.

the aging state and test temperature could be questioned. However, in the specific test conditions used in this work (constant T and T_A during the test), the used expressions and data reduction methods are still applicable. In Fig. 5b data for specimens aged at higher T_A are not included because master curves were constructed using data in higher temperature range that does not overlap with the region in Fig. 5b.

Next, results related to the shift factor a_A will be presented. Since it is not known how the aging state β depends on the aging temperature T_A and aging time t_A, parametric study was performed. The methodology was described in Section 4.2. The reference point with $\log a_A = 0$ in the following graphs is at t_A = 20min (first data point). In Figure 6, the variability of the shift factor dependence on t_A is illustrated for specimens aged at $T_A = 80^{\circ}C$ presenting two independent data for the same specimen Sp10 (annealing after the first program). The results after annealing almost coincide with the previous.

The $\log a_A$ change with t_A in Fig 6b is rather linear in the range $20 < t_A < 700$ min and almost independent on the aging temperature T_A. The rate independence on T_A was observed also in previous works [9,10]. In this interval a single aging temperature independent equation describing the dependence of $\log a_A$ on t_A can be obtained

$$\log a_A = 0.8169 \cdot \log t_A - 1.0735,\ 20 < t_A < 700 \text{ min} \quad (11)$$

Contrary to previously reported results [9,10], the results reported is this paper for $t_A > 700$min in Fig. 6b show a distinct effect of the aging temperature on $\log a_A$. The shift factor at a given t_A is larger if T_A is higher and the behavior deviates from linear. Predictions, done by extrapolating (11) to much larger region than the one used for fitting are shown in Fig. 6b by the dotted line.

For low T_A ($70^{\circ}C$,$80^{\circ}C$) the trendline is in good agreement with the experimental data in the whole t_A region. For higher T_A ($T_A \in [90, 110]^{\circ}C$) the dependence is nonlinear and Eq. (11) for $t_A > 700$ min is not applicable. Investigations at even higher T_A are required to quantitatively describe the nonlinear behavior.

5.3. Predictions at different aging states using sp 11 as a reference

First, the incremental VisCoR code was used to simulate isothermal L-H tests at temperature $T = T_A$corresponding to different aging times t_A at same T_A. Prony coefficients from testing at one selected value of t_{A0} were used to predict the VE behavior in a test with a different t_A. The shift factor changes $\Delta \log a_A$ between these two aging times was calculated using (11). Since the test time was always much shorter than the t_A, a constant shift factor corresponding to the beginning of the test was used.

In Fig. 7a Sp10 aged at $T_A = 80^{\circ}$C for $t_{A0} = 78$ min was used to predict the VE behavior of it after a longer aging time $t_A = 1953$ min. The VE stress data after $t_{A0} = 78$ min was used to find Prony coefficients. The shift between 78 min and 1953 min aging is $\Delta \log a_A = 0.8169 \cdot \log \frac{1953}{78} = 1.143$. In simulations the dependence of the applied strain on time was always taken from the recorded experimental data. Results and data show an excellent agreement. The stress scale is adapted for better revealing the similarities and differences.

Results of a similar procedure for Sp.11 aged and tested at $T = T_A = 90^{\circ}C$ are shown in Fig. 7b. The VE behavior after $t_A = 8177$ min is simulated using Prony coefficients obtained fitting L-H data after sorter aging, $t_{A0} = 301$ min. In this case, using (11) the agreement is not good and the simulated curve, see the dotted line in Fig. 7b, is significantly

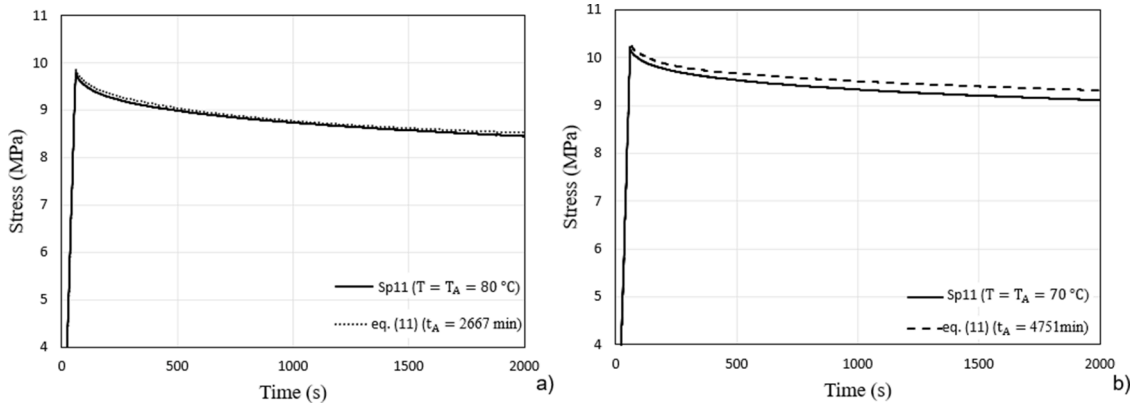

Fig. 8. Stress response in L-H test with $\varepsilon_0 = 0.5\%$ at different aging states. Prony coefficients of the master curve for "A-ref" Sp11 ($T_A = 80^{\circ}C$,$t_A = 8177$ min) were used to simulate tests at different T_A and t_A for a) $T_A = 80^{\circ}$C and b) $T_A = 70^{\circ}$C. Shift factor corresponding to t_A change was calculated using (11).

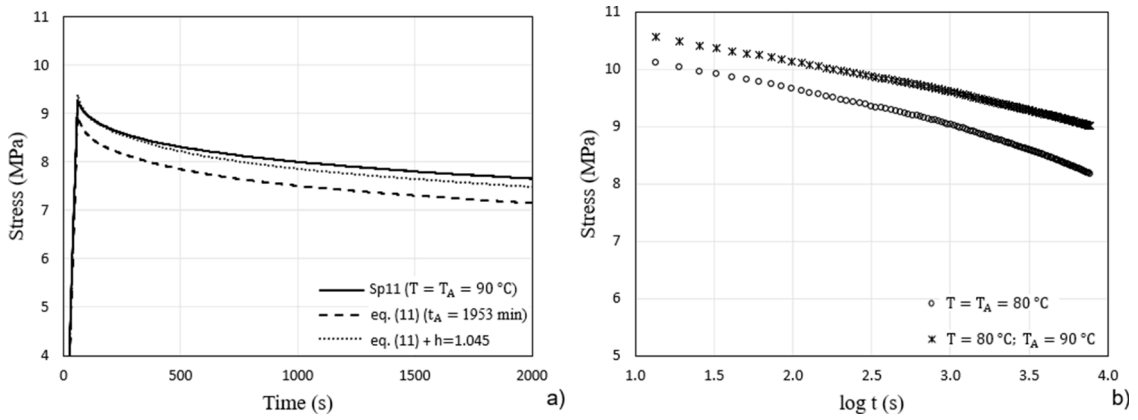

Fig. 9. Effect of T_A on the stress response for Sp11 for a) L-H test ($\varepsilon_0 = 0.5\%$), simulated using master curve Prony coefficients for "A-ref" Sp11 aged at T_A=80 °C for A was calculated using (11) and b) relaxation curves ($\varepsilon_0 = 0.5\%$) at T=80 °C for "A-ref" specimens aged at T_A=80 and 90 °C.

below the experimental. The problem lays in inaccuracy of (11) when used for $T_A = 90°C$ or higher. If, the experimental shift factor change is used, see Fig. 6, $\Delta \log a_A = 1.538$, the agreement with test is much better, except the response during the first minute. The reason for this short-term problem is the rather large value of the shift factor. As high temperature tests cannot be used to predict the short-term response at much lower temperatures, similarly the experimental data from less aged specimens are not suitable for predicting the short-term response of much more aged specimens. This problem was less noticeable in the case shown in Fig. 7a because the shift factor change between 78 min and 1953 min aging was smaller. These results emphasize the necessity to have a better shift factor expression for high aging temperatures than (11).

Simulating results in Fig. 8 and Fig. 9a, the master curve at $T_{ref} = 80°C$ obtained using "A-ref" Sp11 specimen aged at $T_A = 80°C$ was used to find Prony coefficients. In Fig. 8a the Prony coefficients and the temperature shift factor was used to predict the stress response at the same temperature $T = 80°C$ but after aging for $t_A = 2667$ min. Using the master curve, the accuracy is excellent over the whole-time interval. Accuracy is good also in Fig. 8b where the same specimen was rejuvenated and then aged at $T_A = 70°C$ for 4751 min and tested at $T = 70°C$. The a_T values used in simulations in Fig. 8b were obtained during master curve's construction for the Sp11 specimen aged at $T_A = 80°C$. In general, problems with accuracy in the short-term region are not encountered if predictions are done for lower temperatures than the reference and for less aged specimen than the reference aging state. In these cases, the logarithms of temperature and aging shift factors have different signs and partially compensate each other.

Next, the Prony coefficients and shift factors for "A-ref" Sp11 aged at 80°C are used to predict the stress response in L-H test for the same specimen aged at $T_A = 90°C$. Stress predictions in test after aging for t_A=1953 min are shown in Fig. 9a. The curve simulated with (11) is systematically below the experimental. According to Fig. 9b, it is not just due to inaccuracy of (11) for higher T_A. Indeed, the simulated stress relaxation curves at $T = 80°C$ for two aging cases are different: a) "A-ref" aged specimen at $T_A = 80°C$; b) the same "A-ref" specimen aged at $T_A = 90°C$. Since in both cases the specimen is aged to "A-ref" state and tested at the temperature $T = 80°C$, the response should be the same. Nevertheless, stresses for the specimen aged at $90°C$ are higher. Even taking a much higher (unrealistic with respect to data in Fig. 6b) a_A value, assuming that at $T_A = 90°C$ the specimen in the "A-ref" state is aged more, would not solve the problem because the slope of the two curves is also different. This would imply that coefficients in Prony series for "A-ref" specimens depend on the aging temperature, which is impossible in the framework of the used model.

The conclusion is that the T-A-R simple model has limitations. In a T-A-R complex model the temperature and aging dependence may be included in two functions, h_1 and h_2, see (12), similarly as in [22] the degree of cure was included in the viscoelastic model.

$$\sigma(t) = E_r(\beta, T)\varepsilon + h_1(\beta, T)\int_0^t \Delta C(\psi - \psi')\frac{d(h_2(\beta, T)\varepsilon)}{d\psi'}d\psi' \tag{12}$$

In an ideal relaxation test, from the (12) follows

$$\sigma_{rel} = \varepsilon_0\left[E_r + h_1 h_2 \sum_m C^m exp\left(-\frac{\psi}{\tau_m}\right)\right], \quad \psi = \frac{t}{a_A a_T} \tag{13}$$

Since the rubbery modulus E_r is very small, (13) implies that the glassy modulus and the stress curves are proportional to $h = h_1 \bullet h_2$. If so, the ratio of stress at an arbitrary selected time instant in Fig. 9b can be used to find h. As an example, the stress in both curves at $t = 12s$ in Fig. 9b was used, finding $h = 1.045$. This value was used in the VisCoR Model for the rheologically complex case [22], simulating the "eq. (11) + h=1.045" curve in Fig. 9a which is in good agreement with the experimental curve.

These results indicate that the rheological behavior of the epoxy as related to both the temperature and aging may actually be more complex than the T-A-R simple model describes.

In literature, the thermo-rheological complexity in polymeric materials is often described as a phenomenon at extreme temperature and aging conditions when the relaxation times τ_m of a material (the viscoelastic spectrum) are not equally affected by the change in temperature [27]. Therefore, a simple time-temperature superposition with a unique value of activation energy is not possible. The "weight" of each relaxation mechanism could also be changing.

In the terminology used in this paper, the temperature and aging related shift factor would be different for different exponents in Prony series. Each Prony coefficient would have a different multiplier that depends on temperature and aging time. Hence, construction of a master curve using TTSP is not possible [28]. However, the TTSP concept has been applied for two-phase systems, which have two relaxation regimes with two different temperature sensitivities, such as crystalline and semi-crystalline polymers [17–20].

Since the above formulation with different shift and "weight" factors is not compatible with the thermodynamics-based derivation of the Schapery's equations, a different model may be required. In this research, see (12), a simplified approach to account for the complexity (may be sufficiently accurate for "moderate regimes) generalizing Schapery's model and keeping the same test methodology, is outlined: use of a single but more complex form of loga(T, T_A,t_A,t) and a single "average weight factor" h in the VE model.

Therefore, it was shown that splitting the shift factor in two terms related to the test temperature and the aging effect, respectively, is a useful approximation with limitations. However, to obtain predictions

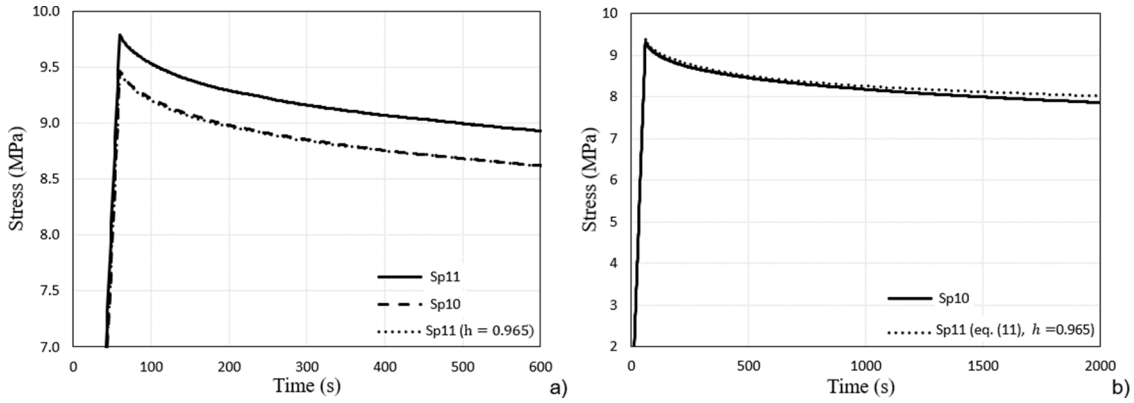

Fig. 10. Stress predictions for Sp10 in L-H test with $\varepsilon_0 = 0.5\%$ using data for Sp11 a) test data for Sp10 and Sp11both aged for 2650 min at $T_A = 80^{\circ}C$ and tested at $80^{\circ}C$ and the Sp11 curve multiplied by $h = 0.965$, b) data for Sp10 aged at $80^{\circ}C$ for $t_A = 1239$ min and tested at $80^{\circ}C$ together with VisCoR simulations using master curve for "A-ref" Sp11 + eq. (11) aged at the same temperature and with $h = 0.965$.

accurately describing the aging effect, a thermo-aging-rheologically complex model may be necessary.

5.4. On variability between different specimens

This Section addresses the problem with VE testing of many specimens at different testing temperatures, aging temperatures and aging times that is very time-consuming. To save time, at each aging temperature L-H tests for 10 min or less could be performed on several specimens followed by a full VE analysis on only one or two of them using the methodology described in this paper.

The hypothesis is that most of the differences in the VE behavior between different specimens are revealed already in the first minutes of the test and they can be used to estimate the scatter between specimens in the long-term VE behavior. For example, the different values of the stress maximum for the two specimens in Fig. 10a result from the VE response in the L-step. These values reflect the effect of all Prony exponents that are actively contributing to predictions in this time interval. This also means that the ratio $\frac{\sigma^{Sp10}_{0.5\%}}{\sigma^{Sp11}_{0.5\%}} = 0.965$ in Fig. 10a for the two specimens, which are in the same test conditions and aging state, reflects differences in their VE behavior. The hypothesis, then, is that all Prony coefficients are affected in approximately the same way, which is consistent with (12) and (13) where a common factor h_1h_2 was introduced. Using $h = h_1h_2 = 0.965$ and knowing a long-time response for Sp11, reliable predictions for another specimen (Sp10) can be made in the same time interval. Perfect agreement is obtained not only for the maximum value but also over the entire time region. Fig 10b shows that using in the VisCoR code $h = 0.965$, parameters for "A-ref" aged Sp11 and shift factors (eq. (11)), it is possible to predict the behavior of Sp10 even at totally different aging state.

6. Conclusions

The effect of physical aging on the viscoelastic (VE) response of a commonly used epoxy resin was investigated using a Schapery's type of VE model, initially assuming that the polymer is thermo-aging-rheologically simple. The VE response was measured in tensile tests at different temperatures for specimens subjected to different aging temperatures T_A and aging times t_A. It was demonstrated that very reliable and repeatable results and trends are obtained if the same specimen is used over the entire testing program, without removing it from the testing machine, and if the same program is repeated after thermal rejuvenation. In the presented model, the shift factor is presented as a product of two independent terms: one responsible for different test temperatures and the other responsible for any possible changes in the aging state. Specimens sufficiently aged to ensure constant aging state during tests at different temperatures were used for master curve construction and determination of shift factors.

The results show that in the first 700 min of aging, the aging shift factor change with t_A is similar for all T_A. The relationship, described with a linear fitting function in logarithmic axes, renders good accuracy of simulations. However, with increasing aging time the effect of the T_A becomes noticeable; the aging shift factor changes faster at higher T_A. The temperature shift factors for specimens aged for a long time also depend on aging temperature. Comparing relaxation curves at the same temperature for specimens aged for the same long time at two different high T_A, the stress is higher and the slope is smaller if the T_A is higher.

These facts imply that a thermo-aging-rheologically complex model must be developed for improved predictions. It should include new aging dependent parameters in addition to the shift factor.

Declaration of Competing Interest

The authors declare that they have no known competing financial interests or personal relationships that could have appeared to influence the work reported in this paper.

Acknowledgements

The authors would like to thank Higher Education Improvement Coordination (CAPES/Brazil), The Swedish Foundation for International Cooperation in Research and Higher Education (STINT), Kempestiftelserna with funding referens SMK-1738 and ERDF within the Activity 1.1.1.2 "Post-doctoral Research Aid" of the Specific Aid Objective of the Operational Programme "Growth and Employment" (project No. 1.1.1.2/VIAA/4/20/641) for their financial support.

References

[1] D. Cangialosi, V.M. Boucher, A. Alegría, J. Colmenero, Physical aging in polymers and polymer nanocomposites: recent results and open questions, Soft Matter 9 (2013) 8619–8630.
[2] S. Montserrat, P. Cortés, A.J. Pappin, K.H. Quah, J.M. Hutchinson, Structural relaxation in fully cured epoxy resins, J. NonCryst. Solids 172-174 (1994) 1017–1022.
[3] G.M. Odegard, A. Bandyopadhyay, Physical aging of epoxy polymers and their composites, J. Polym. Sci. B Polym. Phys. 49 (2011) 1695–1716.
[4] H. Parvatareddy, J.Z. Wang, D.A. Dillard, T.C. Ward, Environmental aging of high-performance polymeric composites: effects on durability, Compos. Sci. Technol. 53 (1995) 399–409.
[5] G.B. McKenna, On the physics required for prediction of long term performance of polymers and their composites, J. Res. Natl Inst. Stand. Technol. 99 (2) (1994) 169–189.
[6] J.C. Arnold, The influence of physical aging on the creep rupture behavior of polystyrene, J. Polym. Sci. B Polym. Phys. 31 (1993) 1451–1458.
[7] V.T. Truong, B.C. Ennis, Effect of physical aging on the fracture behavior of crosslinked epoxies, Polym. Eng. Sci. 31 (8) (1991) 548–557.

[8] C. G'Sell, G.B McKenna, Influence of physical aging on the yield response of model DGEBA/poly(propylene oxide) epoxy glasses, Polymer (Guildf) 33 (10) (1992) 2103–2113.
[9] A. Lee, G.B. McKenna, The physical aging response of an epoxy glass subjected to large stresses, Polymer (Guildf) 31 (1990) 423–430.
[10] L.C.E. Struik, Physical Aging in Plastics and Other Glassy Materials, Polym. Eng. Sci. 17 (3) (1977) 165–173.
[11] J.M. Hutchinson, D. Mccarthy, S. Montserrat, P. Cortés, Enthalpy relaxation in a partially cured epoxy resin, J. Polym. Sci. B Polym. Phys. 34 (1996) 229–239.
[12] I.M. Hodge, Physical aging in polymer glasses, Science 267 (1995) 1945–1947.
[13] S. Vleeshouwers, A.M. Jamieson, R. Simha, Effect of physical aging on tensile stress relaxation and tensile creep of cured epon 828/epoxy adhesives in the linear viscoelastic region, Polym. Eng. Sci. 29 (10) (1989) 662–670.
[14] M.M. Santore, R.S. Duran, G.B. McKenna, Volume recovery in epoxy glasses subjected to torsional deformations: the question of rejuvenation, Polymer (Guildf) 32 (13) (1991) 2377–2381.
[15] Barbero E.J. Time-temperature-age superposition principle for predicting long-term response of linear viscoelastic materials. In: Guedes RM, editor. Creep and Fatigue in Polymer Matrix Composites: Woodhead Publishing, 2019. p.66–86.
[16] G.B. McKenna, Physical Aging in Glasses and Composites, editors, in: KV Pochiraju, GP Tandon, GA Schoeppner (Eds.), Long-Term Durability of Polymeric Matrix Composites, Springer, New York, 2012, pp. 237–309.
[17] Y. Guo, R.D. Bradshaw, Long-term creep of polyphenylene sulfide (PPS) subjected to complex thermal histories: the effects of nonisothermal physical aging, Polymer (Guildf) 50 (2009) 4048–4055.
[18] M.H.M. Dias, K.M.B. Jansen, J.W. Luinge, H.E.N. Bersee, R. Benedictus, Effect of fiber-matrix adhesion on the creep behavior of CF/PPS composites: temperature and physical aging characterization, Mech. Time Depend. Mater. 20 (2016) 245–262.
[19] E.R. Pierik, W.J.B. Grouve, M. van Drongelen, R. Akkerman, The influence of physical aging on the in-plane shear creep compliance of 5HS C/PPS, Mech. Time Depend. Mater. 24 (2020) 197–220.
[20] R.D. Bradshaw, L.C. Brinson, Physical aging in polymers and polymer composites: an analysis and method for time-aging time superposition, Polym. Eng. Sci. 37 (1) (1997) 31–44.
[21] R.A. Schapery, Nonlinear viscoelastic and viscoplastic constitutive equations based on thermodynamics, Mech. Time-Depend Mater 1 (1997) 209–240.
[22] S. Saseendran, D. Berglund, J. Varna, Viscoelastic model with complex rheological behavior (VisCoR): incremental formulation, Adv. Manuf. Polym. Compos. Sci. 6 (1) (2020) 1–16.
[23] S. Saseendran, D. Berglund, J. Varna, Stress relaxation and strain recovery phenomena during curing and thermomechanical loading: thermorheologically simple viscoelastic analysis, J. Compos. Mater. 53 (26–27) (2019) 3841–3859.
[24] B. Bolasodun, O. Rufai, A. Nesbitt, R. Day, Comparison of the isothermal cure kinetics of Araldite LY 5052/4 4'DDS epoxy system using a differential scanning calorimetry and a microwave heated calorimeter, Int. J. Mater. Eng. 4 (4) (2014) 148–165.
[25] S.G. Nunes, S. Saseendran, R. Joffe, S.C. Amico, P. Fernberg, J. Varna, On temperature-related shift factors and master curves in viscoelastic constitutive models for thermoset polymers, Mech. Compos. Mater. 56 (5) (2020) 573–590.
[26] Fukushima K., Cai H., Nakada M., Miyano Y. Determination of time-temperature shift factor for long-term life prediction of polymer composites. In: Proceedings of ICCM17–17th International Conference On Composite Materials. Edinburgh, July 2009. p.1–9.
[27] Z. Yan, F.J. Stadler, Classification of thermorheological complexity for linear and branched polyolefins, Rheol. Acta 57 (2018) 377–388.
[28] N. Heymans, Constitutive equations for polymer viscoelasticity derived from hierarchical models in cases of failure of time–temperature superposition, Signal Process. 83 (2003) 2345–2357.